Inhomogeneous charge states and electronic transport in manganites

Kagan, M.Y.; Kugel, K.I.; Rakhmanov, A.L.; Khomskii, D.I

Published in:
Low Temperature Physics

DOI:
10.1063/1.1399195

Publication date:
2001

Fizika Nizkikh Temperatur, 2001, v. 27, No. 8, p. 815–825

Inhomogeneous charge states and electronic transport in manganites

(Review Article)

M. Yu. Kagan[1], K. I. Kugel[2], D. I. Khomskii[3], and A. L. Rakhmanov[2]

[1] *P. L. Kapitza Institute for Physical Problems, Russian Academy of Sciences*
2 Kosygina Str., 117334 Moscow, Russia
E-mail: kagan@kapitza.ras.ru

[2] *Institute of Theoretical and Applied Electrodynamics, Russian Academy of Sciences*
13/19 Izhorskaya Str., 127412 Moscow, Russia

[3] *Laboratory of Applied and Solid State Physics, Materials Science Center, University of Groningen*
Nijenborgh 4, 9747 AG Groningen, The Netherlands

Received February 9, 2001

We analyze the interplay between charge ordering, magnetic ordering, and the tendency toward phase separation and its importance for the physics of manganites. A simple model of charge ordering is considered. It takes into account both the Coulomb repulsion at neighboring sites responsible for charge ordering and the essential magnetic interactions. It is shown explicitly that at any deviation from half-filling ($n \neq 1/2$) the system is unstable with respect to phase separation into charge-ordered regions with $n = 1/2$ and metallic regions with smaller electron or hole density. A possible structure of this phase-separated state (metallic droplets in a charge-ordered matrix) is discussed. We construct the phase diagram reproducing the main features observed in real manganites. Based on the same physical picture, we also derive explicit expressions for the dc conductivity and noise power in the phase-separated state. It is shown that the noise spectrum has nearly $1/f$ form in the low-frequency range.

PACS: **64.75.+g**, **71.27.+a**, **71.30.+h**, **72.10.−d**, **72.70.+m**, 75.30.Vn

Contents

1. Introduction

The problem of charge ordering in magnetic oxides has attracted the attention of theorists since the discovery of the Verwey transition in magnetite at the end of thirties [1]. Recently this problem has been reexamined in a number of papers in connection with the colossal magnetoresistance in manganites; see, e.g., [2–4]. The mechanisms stabilizing the charge-ordered (CO) state may be different: the Coulomb repulsion of charge carriers or the electron-lattice interaction leading to the effective, repulsion of electrons at the nearest neighbor sites. In all cases, charge ordering can arise in systems with mixed valence if the electron bandwidth is sufficiently small — large electron kinetic energy stabilizes the homogeneous metallic state. In the simplest bipartite lattice, the class which includes the colossal magnetoresistance manganites of the type

$R_{1-x}A_xMnO_3$ (R = La, Pr; A = Ca, Sr) or layered manganites $R_{2-x}A_xMnO_4$, $R_{2-2x}A_{1+2x}Mn_2O_7$, the optimum conditions for the formation of the CO state exist for doping $x = 1/2$. At this value of x the concentrations of Mn^{3+} and Mn^{4+} are equal, and a simple checkerboard arrangement is possible. The most remarkable experimental fact here is that even at $x \neq 1/2$ (in the underdoped manganites, $x < 1/2$) only the simplest version of charge ordering is experimentally observed, with an alternating checkerboard structure of occupied and empty sites in the basal plane [5].

Then the natural question arises: how could we redistribute the extra or missing electrons in the case of arbitrary doping level, keeping the superstructure the same as for $x = 1/2$? To answer this question, the experimentalists introduced the concept of an incipient charge-ordered state corresponding to the distortion of long-range charge ordering by microscopic metallic clusters [6]. In fact, the existence of such a state implies a kind of phase separation. Note that the phase separation scenario in manganites is very popular now [7–10]. Nowadays, there is a growing evidence suggesting that an interplay between the charge ordering and the tendency toward phase separation plays an essential role in the physics of materials with colossal magnetoresistance.

In this paper we consider a simple model which allows us to clarify the situation at arbitrary doping. We include in this model both the Coulomb repulsion of electrons on neighboring sites and the magnetic interactions responsible for the spin ordering of manganites. After demonstrating the instability of the system toward phase separation in certain ranges of doping, we consider the simplest form of the phase separation — the formation of metallic droplets in an insulating matrix, estimate parameters of such droplets, and construct the phase diagram illustrating the interplay between charge ordering, magnetic ordering, and phase separation.

Based on this model, we also calculate the conductivity and noise spectral power of the system in the phase-separated state, taking into account the electron jumps from one droplet to another. The concentration range not too close to the percolation transition to the metallic state is considered. The relation of these results to the giant $1/f$ noise observed in the phase-separated manganites [11] is discussed.

2. A simple model for charge ordering

Let us consider a simple lattice model for charge ordering:

$$\hat{H} = -t \sum_{<i,j>} c_i^+ c_j + V \sum_{<i,j>} n_i n_j - \mu \sum_i n_i , \quad (1)$$

where t is the hopping integral, V is the nearest neighbor Coulomb interaction (similar *nn* repulsion can be also obtained via the interaction with the breathing-type optical phonons); μ is the chemical potential, and c_i^+ and c_j are one-electron creation and annihilation operators, $n_i = c_i^+ c_i$. The symbol $\langle i, j \rangle$ denotes the summation over the nearest-neighbor sites. Here, for simplicity, we omit the spin indices. We also assume the absence of double occupancy in this model due to the strong on-site repulsion between electrons.

Models of the type (1) with the *nn* repulsion being responsible for the charge ordering are the most popular ones for describe this phenomenon; see, e.g., [2,4,12–14] and references therein. Hamiltonian (1) captures the main physical effects; if necessary, one can add to it some extra terms, which we will also do below.

In the main part of our paper, we will always speak about electrons. However, in application to real manganites we will mostly have in mind less-than-half-doped (underdoped) systems of the type $R_{1-x}A_xMnO_3$ with $x < 1/2$. Thus, for a real system one has to substitute *holes* for our *electrons*. All the theoretical treatment definitely remains the same (from the very beginning we could define operators c and c^+ in (1) as the operators for holes); we hope that it will not lead to any misunderstanding.

We consider below the simplest case of square (2D) or cubic (3D) lattices, where for $x = 1/2$ the simple two-sublattice ordering would take place. As mentioned in the Introduction, this is the case in layered manganites, whereas the ordering in 3D perovskite manganites is like this only in the basal plane, the ordering being «in-phase» in the c direction. To account for this behavior, apparently a more complicated model would be necessary.

For the case $n = 1/2$, model (1) has been analyzed in many papers; we follow the treatment of Ref. 12 (see also [10]). As mentioned above, the Coulomb repulsion (the second term in (1)) stabilizes the charge ordering in the form of a checkerboard arrangement of occupied and empty sites, whereas the first term (band energy) opposes this tendency. At arbitrary values of electron density n, we shall at first consider a homogeneous CO solution and use the same ansatz as in [12], namely

$$n_i = n\,[1 + (-1)^i\,\tau]\ . \qquad (2)$$

Such an expression implies the doubling of lattice periodicity, with the local densities $n_1 = n(1 + \tau)$ and $n_2 = n(1 - \tau)$ at neighboring sites. Note that at $n = 1/2$ for a general form of electron dispersion without nesting, the CO state exists only at sufficiently strong repulsion $V > 2t$ [12]. For finite values of $V/2t$ the order parameter $\tau < 1$, and the ordering in general is not complete, i.e., the average electron densities n_i differ from zero or one even at $T = 0$.

We use the same coupled Green function approach as in [12], which leads to the following spectrum:

$$E + \mu = Vnz \pm \sqrt{(Vn\tau z)^2 + t_k^2} = Vnz \pm \omega_k\ . \qquad (3)$$

The spectrum defined by (3) resembles the spectrum of a superconductor, and hence the first term under the square root is analogous to the superconducting gap squared. In other words, we can introduce the charge-ordering gap by the formula $\Delta = Vn\tau z$. It depends upon density not only explicitly, but also via the density dependence of τ.

Hence, we get

$$\omega_k = \sqrt{\Delta^2 + t_k^2}\ . \qquad (4)$$

Note that there is one substantial difference between the spectrum of the charge ordered state (4) and superconducting state, namely, here for $n \neq 1/2$ the chemical potential does not appear under the square root in (4), in contrast to the spectrum of superconductor, where $\omega_k = [(t_k - \mu)^2 + \Delta^2]^{1/2}$. Thus, the problem of the uniform CO state is reduced to a self-consistent determination of the gap Δ and chemical potential μ as functions of charge density n and temperature:

$$2n = \int \frac{d^3\mathbf{k}}{\Omega_{BZ}}\,[f_F(\varepsilon_{k-}) + f_F(\varepsilon_{k+})]\ ,$$
$$1 = \frac{Vz}{2}\int \frac{d^3\mathbf{k}}{\Omega_{BZ}}\,\frac{1}{\omega_k}\,[f_F(\varepsilon_{k-}) - f_F(\varepsilon_{k+})]\ , \qquad (5)$$

where $f_F(\varepsilon_{k\pm}) = 1/(\exp\{\varepsilon_{k\pm}/T\} + 1)$ are the Fermi distribution functions, and Ω_{BZ} is the volume of the first Brillouin zone. The first equation in (5) determines the chemical potential and the second one gives the gap Δ. For low temperatures $T \to 0$ and $n \leq 1/2$ it is reasonable to assume that $\mu - Vnz$ is negative. Hence $f_F(\omega_k - \mu + Vnz) = 0$, and $f_F(-\omega_k - \mu + Vnz) = \theta(-\omega_k - \mu + Vnz)$ is the step function.

It is easy to see that for $n = 1/2$ the system of equations (5) yields identical results for all $-\Delta \leq \mu - Vnz \leq \Delta$. From this point of view, $n = 1/2$ is a point of indifferent equilibrium. For infinitely small deviations from $n = 1/2$, that is, for densities $n = 1/2 - 0$, the chemical potential should be defined as $\mu = -\Delta + Vz/2 = Vz/2(1 - \tau)$. If we consider the strong-coupling case $V >> 2t$ and assume a constant density of states inside the band, then for a simple cubic lattice we have $\tau = 1 - (2W^2/3V^2z^2)$, and hence

$$\mu = \frac{W^2}{3Vz}\ , \qquad (6)$$

where $W = 2zt$ is the bandwidth. Note that for density $n = 1/2$ a charge-ordering gap Δ appears for an arbitrary interaction strength V. This is due to the existence of nesting in our simple model. In the weak coupling case $V << 2t$ and with perfect nesting, we have $\Delta \sim W \exp\{-W/Vz\}$, and τ is exponentially small. For $zV >> W$ or, accordingly, for $V >> 2t$: $\Delta \approx Vz/2$ and $\tau \to 1$. As mentioned above, for a general form of electron dispersion without nesting, charge ordering exists only if the interaction strength V exceeds a certain critical value of the order of the bandwidth W [12]. Further on, we restrict ourselves only to the physically more instructive case of strong coupling $V >> 2t$.

Now let us consider the case $n = 1/2 - \delta$, where $\delta << 1$ is a deviation from density $n = 1/2$. For this case $\mu = \mu(\delta, \tau)$, and we have two coupled equations for μ and τ. As a result,

$$\mu(\delta) \approx Vnz(1 - \tau) - \frac{4W^2}{Vz}\,\delta^2 \approx$$
$$\approx \frac{W^2}{3Vz} + \frac{4W^2}{3Vz}\,\delta + O(\delta^2)\ . \qquad (7)$$

Correspondingly, the energy of a charge ordered state is as follows

$$E_{CO}(\delta) = E_{CO}(0) - \frac{W^2}{3Vz}\,\delta - \frac{2W^2}{3Vz}\,\delta^2 + O(\delta^3)\ , \qquad (8)$$

where $E_{CO}(0) = -W^2/6Vz$ is the energy of charge-order for density n precisely equal to $1/2$ and $|E_{CO}(0)| << W$. At the same time, the charge-ordering gap Δ is given by:

$$\Delta \approx \frac{Vz}{2}\left[1 - 2\delta - \frac{2W^2}{3V^2z^2}\,(1 + 4\delta)\right]. \qquad (9)$$

For $n > 1/2$ the energy of the charge-ordered state starts to increase rapidly due to the large contribution from the Coulomb repulsion (the upper Verwey band is partially filled for $n > 1/2$). Contrary to the case $n < 1/2$, for $n > 1/2$ each extra electron put into the checkerboard CO state will necessarily have occupied nearest-neighbor sites, increasing the total energy by $Vz|\delta|$. As a result, we have for $|\delta| = n - 1/2 > 0$

$$E_{CO}(\delta) = E_{CO}(0) + \left(Vz - \frac{W^2}{3Vz} \right) |\delta| - \frac{2W^2}{3Vz} \delta^2 + O(\delta^3) . \quad (10)$$

Accordingly, the chemical potential has the form

$$\mu(\delta) = Vz - \frac{W^2}{3Vz} - \frac{4W^2}{3Vz} |\delta| + O(\delta^2) . \quad (11)$$

It undergoes a jump equal to Vz for $\tau \to 1$. Note that the gap Δ is symmetric for $n > 1/2$ and is given by

$$\Delta \approx \frac{Vz}{2} \left[1 - 2|\delta| - \frac{2W^2}{3V^2z^2} (1 + 4|\delta|) \right] .$$

We could make the whole picture symmetric with respect to $n = 1/2$ by shifting all the one-electron energy levels and the chemical potential by $Vz/2$, i.e., defining $\mu' = \mu - Vz/2$. In terms of μ', relations (7), and (11) can be written as:

$$\mu' = -\frac{Vz}{2} + \frac{W^2}{3Vz} + \frac{4W^2}{3Vz} \delta , \; n < \frac{1}{2} ;$$

$$\mu' = \frac{Vz}{2} - \frac{W^2}{3Vz} - \frac{4W^2}{3Vz} |\delta| , \; n > \frac{1}{2} .$$

Similar to the situation in semiconductors, here $\mu' = 0$ precisely at the point $n = 1/2$, i.e., the chemical potential lies in the middle of the band gap (see Fig. 1). At densities $n = 1/2 - 0$, the chemical potential $\mu' = -Vz/2$ coincides with the upper edge of the filled Verwey band.

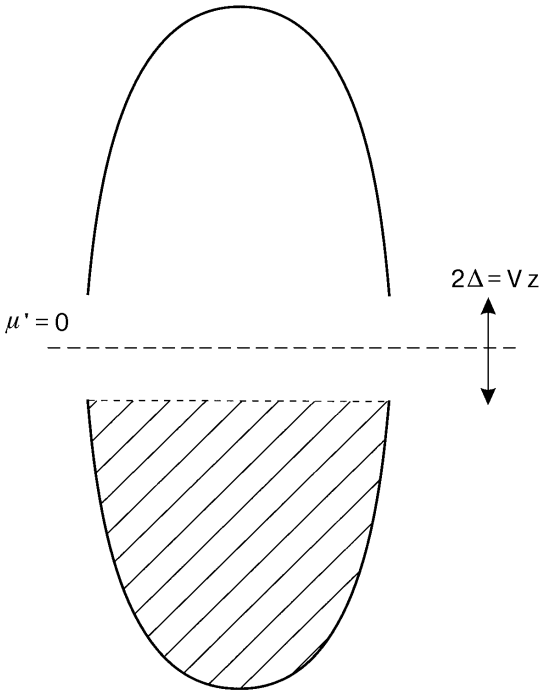

Fig. 1. Band structure of the model (1) at $n = 1/2$. The lower Verwey band is completely filled. The upper Verwey band is empty. The chemical potential $\mu' = 0$ lies in the middle of the band gap of the width 2Δ.

3. Phase separation

Let us check now the stability of the charge-ordered state. At densities close to $n = 1/2$, the dependence of the energy on charge density will have the form illustrated in Fig. 2.

This figure is clearly indicative of possible instability of the charge ordered state. Indeed, the most remarkable implication of (7)–(11) is that the compressibility κ of the homogeneous charge-ordered system is negative for densities different from 1/2,

$$\frac{1}{\kappa} \propto \frac{d\mu}{dn} = \frac{d\mu}{d\delta} = \frac{d^2E}{d\delta^2} = -\frac{4W^2}{3Vz} < 0 , \quad (12)$$

where $\delta = 1/2 - n$. This is a manifestation of the tendency toward phase separation characteristic of the charge-ordered system with $\delta \neq 0$. The presence of a kink in $E_{CO}(\delta)$ (cf. Eqs. (8), (10)) implies that one of the states into which the system might separate would correspond to the checkerboard CO state with $n = 1/2$, whereas the other would have a certain density n' smaller or larger than 1/2. This conclusion resembles that of [3] (see also [9,15]), although the detailed physical mechanism is diffe-

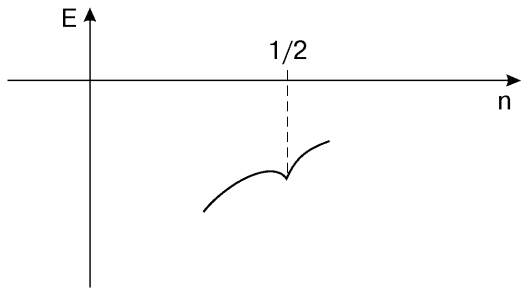

Fig. 2. Energy of the charge-ordered state versus charge density at $n \to 1/2$.

rent. The possibility of the phase separation in the model (1) away from half-filling was also reported earlier in [13] for the infinite-dimensional case. Below we concentrate our attention on the situation with $n < 1/2$ (underdoped manganites); the case $n > 1/2$ apparently has certain special properties — the existence of stripe phases etc. [16], the detailed origin of which is not yet clear.

It is easy to understand the physics of phase separation in our case. As follows from (9), the CO gap decreases linearly with the deviation from the half-filling. Correspondingly, the energy of the homogeneous CO state increases rapidly, and it is more favorable to «extract» extra holes from the CO state, putting them into one part of the sample, while creating the «pure» checkerboard CO state in the other part of it. The energy cost of such a redistribution of holes is overcompensated by the energy benefit provided by the better charge ordering.

The long-range Coulomb forces would, however, prevent the full phase separation into large regions containing all extra holes and the pure $n = 1/2$ charge ordered region. We can avoid this energy cost by forming finite metallic clusters with a smaller number of electrons instead of one big metallic phase with many electrons. The limiting case would be a set of spherical droplets, each containing one electron. This state is similar to magnetic polarons («ferrons») considered in the problem of phase separation in doped magnetic insulators [7,15,10].

We present below an estimation of the characteristic parameters of these droplets. The main aim of this treatment is to demonstrate that the state constructed in such a way will have lower energy than the homogeneous state, even if we treat these droplets rather crudely and do not optimize all their properties. In particular, we will make the simplest assumption that the droplets have sharp boundaries and that the charge-ordered state outside these droplets is not modified in their vicinity. This state can be treated as a variational one: if we optimize the structure of the droplet boundary, its energy would only decrease.

The energy (per unit volume) of the droplet state with a concentration n_d of the droplets can be written in total analogy with the ferron energy in the double-exchange model (see [10,15]). This yields

$$E_{\text{droplet}} = -tn_d\left(z - \frac{\pi^2 a^2}{R^2}\right) - \frac{W^2}{6Vz}\left[1 - n_d\,\frac{4}{3}\,\pi\left(\frac{R}{a}\right)^3\right]. \tag{13}$$

Here a is the lattice constant and R is the droplet radius. The first term in (13) corresponds to the kinetic energy benefit of electron delocalization inside the metallic droplets, and the second term describes the charge ordering energy in the remaining insulating part of the sample.

Minimization of the energy in (13) with respect to R gives

$$\frac{R}{a} \approx \left(\frac{2V}{t}\right)^{1/5}. \tag{14}$$

The critical concentration n_{dc} corresponds to the configuration where metallic droplets start to overlap, i.e., where the volume of the CO phase (the second term in (13)) tends to zero. Hence,

$$n_{dc} = \frac{3}{4\pi}\left(\frac{a}{R}\right)^3 \propto \left(\frac{t}{V}\right)^{3/5}. \tag{15}$$

Actually, one should include the surface energy contribution to the total energy of the droplet. The surface energy should be of the order of W^2R^2/V. For large droplets, this contribution is small compared to the term $\propto R^3$ in (13); it would also be reduced for a «soft» droplet boundary. It is easy to show that even in the worst case of a small droplet (of the order of several lattice constants) with the sharp boundary, R/a acquires a factor $1 - 0.2(t/2V)^{1/5}$ related to the surface contribution. Thus, the corrections related to the surface would not exceed about 20% of the bulk value. That is why we will ignore this term below.

By comparing (8) with (13), we see that for deviations from half-filling, $0 < \delta \le \delta_c = 1/2 - n_{dc}$, the energy of the phase-separated state is always lower than the energy of the homogeneous charge-ordered state. Thus the energy of a phase-separated state with droplets corresponds to the global minima of the energy for all $0 < \delta \le \delta_c$. This justifies our conclusion about phase separation into a charge-ordered state with $n = 1/2$ and a metallic state with small spherical droplets.

Note also that for $n > 1/2$ the compressibility of the charge-ordered state is again negative $1/\kappa = d^2E/d\delta^2 = -4W^2/3Vz < 0$ and has the same value as for the case $n < 1/2$. As a result, it is again more favorable to create a phase-separated state for these densities. However, as we have said, the nature of the second phase with $n > 1/2$ is not quite clear at present, and we shall therefore not consider this case here.

4. An extended model

Now we can extend the model discussed in the previous Sections by taking into account the essential magnetic interactions. In manganites, besides the conduction electrons in e_g bands, there exist also practically localized t_{2g} electrons, which we now include in our consideration. The corresponding Hamiltonian has the form

$$\hat{H} = -t \sum_{<i,j>,\sigma} c^{+}_{i\sigma} c_{j\sigma} + V \sum_{<i,j>} n_i\, n_j -$$

$$- J_H \sum_i \mathbf{S}_i\, \boldsymbol{\sigma}_i + J \sum_{<i,j>} \mathbf{S}_i\, \mathbf{S}_j - \mu \sum_i n_i \quad . \qquad (16)$$

In comparison to (1), the additional terms here correspond to the strong Hund-rule on-site coupling J_H between the localized spins $\mathbf{S}$ and the spins of conduction electrons $\boldsymbol{\sigma}$, and to the relatively weak Heisenberg antiferromagnetic (AFM) exchange J between neighboring local spins. In real manganites, the AFM ordering of the CE type in the CO phase is determined not only by the exchange of localized t_{2g} electrons but to a large extent by the charge- and orbitally-ordered e_g electrons themselves. For simplicity, we ignore this factor here and assume that the superexchange interaction is the same both in the CO and in the metallic phases.

It is physically reasonable to consider this model in the limit

$$J_H S > V > W > JS^2 \; .$$

In the absence of the Coulomb term, this is exactly the conventional double-exchange model (see, e.g., [7,15]). The large Hund's term favors the metallicity in the system, since the effective bandwidth in our problem depends upon the magnetic order. Therefore, the estimate, for the critical concentration here is different from (15). As in [15] the metallic droplets will be ferromagnetic (FM) due to the double exchange. The energy of this state has the form:

$$E = -tn_d \left(z - \frac{\pi^2 a^2}{R^2} \right) - \frac{W^2}{6Vz} \left[1 - \frac{4}{3}\pi \left(\frac{R}{a} \right)^3 n_d \right] +$$

$$+ zJS^2 \frac{4}{3}\pi \left(\frac{R}{a} \right)^3 n_d - zJS^2 \left[1 - \frac{4}{3}\pi \left(\frac{R}{a} \right)^3 n_d \right] . \qquad (17)$$

The last two terms in (17) describe, respectively, the energy cost of the Heisenberg AFM exchange inside the FM metallic droplets and the energy benefit from it in the AFM insulating part of the sample. Minimization with respect to the droplet radius (as in (13)) yields:

$$\frac{R}{a} \propto \left(\frac{t}{V} + \frac{JS^2}{t} \right)^{-1/5} . \qquad (18)$$

Note that for $t/V << JS^2/t$, formula (18) gives just the same estimate for the radius of FM metallic droplet $R/a \sim (t/JS^2)^{1/5}$ as in [7,15].

In the opposite limit, when $t/V >> JS^2/t$, we recover the same result $R/a \sim (V/t)^{1/5}$ as in (14). Finally, the critical concentration n_c is estimated as follows

$$n_c \propto \left(\frac{t}{V} + \frac{JS^2}{t} \right)^{3/5} . \qquad (19)$$

As a result, taking into account also the tendency toward phase separation at very small values of n [7–10,15], we come to the following phase diagram for the extended model (cf. [10]):

1. At $0 < n < (JS^2/t)^{3/5}$ it corresponds to phase separation into a FM metal embedded in an AFM insulating matrix. To minimize the Coulomb energy, it may be again favorable to split this metallic region into droplets with an average radius given by (18) with $t/V = 0$, each droplet containing one electron and kept apart from one another.

2. At $(JS^2/t)^{3/5} < n < (t/V + JS^2/t)^{3/5} < 1/2$, the system is a FM metal.

Of course, we need a window of parameters to satisfy the inequality in the right-hand side. In actual manganites where $t/V \sim 1/2$–$1/3$ and $JS^2/t \sim 0.1$, these conditions upon n are not necessarily satisfied. Experiments suggest that this window is present for $La_{1-x}Ca_xMnO_3$, but it is definitely absent for $Pr_{1-x}Ca_xMnO_3$ [10].

3. Finally, at $(t/V + JS^2/t)^{3/5} < n < 1/2$, we have phase separation in the form of FM metallic droplets inside an AFM charge-ordered matrix.

This phase diagram is in good qualitative agreement with many available experimental results for real manganites [17–20], in particular with the observation of small-scale phase separation close to 0.5 doping [21]. Note also that our phase diagram has certain similarities with the phase diagram obtained in [22,23] for the problem of spontaneous ferromagnetism in doped excitonic insulators.

5. Conductivity of the phase-separated state

Let us consider an insulating antiferromagnetic sample of volume V_s in electric field **E**. The total number of magnetic polarons in the volume is N, and thus their spatial density is $n = N/V_s$. As was mentioned before, the number of polarons is assumed to be equal to the number of charge carriers introduced by doping. Neglecting the conductivity of the insulating phase, we assume that charge carriers are only located within the droplets. Charge transfer can thus occur either due to the motion of droplets or due to electron tunneling. The former mechanism is less effective because of the large effective mass of magnetic polarons and their possible pinning by crystal lattice defects. We therefore neglect the contribution of polaron motion.

A magnetic polaron in the ground state contains one electron. As a result of a tunneling process, droplets with more than one electron are created, and some droplets become empty. If the energy of an empty droplet $E(0)$ is taken to be zero, the energy of a droplet with one electron can be estimated as $E(1) \sim t(a/R)^2$. This is essentially the kinetic energy of an electron localized in a sphere of radius R. In the same way, the energy of two-electron magnetic polaron $E(2) \sim 2E(1) + U$, with U being the interaction energy of the two electrons. In all these estimates, we have disregarded the surface energy, which is expected to be small (see the previous section). Thus, $E(2) + E(0) > 2E(1)$, and the creation of two-electron droplets is associated with an energy barrier of the order of $A \equiv E(2) - 2E(1) \sim U$. It is clear that the interaction energy U of two electrons in one droplet is determined mainly by the Coulomb repulsion of these electrons, hence $A \sim e^2/\varepsilon a$, where ε is the static dielectric constant, which in real manganites can be rather large ($\varepsilon \sim 20$). We assume below that the mean distance between the droplets is $n^{-1/3} >> R$ (the droplets do not overlap). Then A is larger than the average Coulomb energy $e^2 n^{1/3}/\varepsilon$. Since the characteristic value of the droplet radius R is of the order of 10 Å, we have $A/k_B \sim 1000$ K, and $A > k_B T$ in the case under study. In the following, we assume that the temperature is low, $A >> k_B T$, and we do not consider the possibility of the formation of droplets with three or more electrons.

Let us denote the numbers of single-electron, two-electron, and empty droplets as N_1 , N_2 , and N_3 , respectively. According to our model, $N_2 = N_3$, $N_1 + 2N_2 = N$, and N is constant. Before turning to the conductivity, we evaluate the thermal averages of N_1 and N_2 . To this end, we note that the number P_N^m of possible states with m two-electron droplets and m empty droplets is equal to $C_N^m C_{N-m}^m$, where C_N^m are the binomial coefficients. Since the created pairs of droplets are independent, we write the partition function in the form

$$Z = \sum_{m=0}^{N/2} P_N^m \exp(-m\beta) , \quad \beta = A/k_B T . \qquad (20)$$

Approximating the sum by an integral and using Stirling's formula for the factorials, we get

$$Z = \int_0^{N/2} dm \exp\left[-m\beta - N \ln\left(1 - \frac{2m}{N}\right) + 2m \ln\left(\frac{N}{m} - 2\right)\right].$$

Calculating Z in the saddle-point approximation, and subsequently evaluating in the same way the statistical average of N_2 ,

$$\overline{N}_2 = Z^{-1} \sum_{m=0}^{N/2} m P_N^m \exp(-m\beta) = -\frac{\partial}{\partial\beta} \ln Z , \qquad (21)$$

we easily obtain

$$\overline{N}_2 = N \exp(-A/2k_B T) ,$$
$$\overline{N}_1 = N - 2\overline{N}_2 = N\,[1 - 2\exp(-A/2k_B T)] . \qquad (22)$$

Within the framework of the proposed model, the electron tunneling occurs via one of the following four processes illustrated in Fig. 3:

(i) In the initial state we have two droplets in the ground state, and after tunneling in the final state we have an empty droplet and a droplet with two electrons;

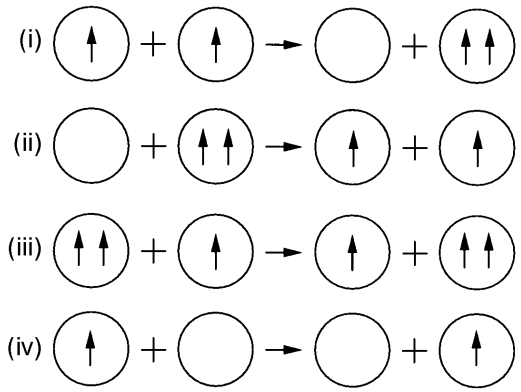

Fig. 3. Elementary tunneling processes.

(ii) An empty droplet and a two-electron droplet in the initial state transform into two droplets in the ground state (two droplets with one electron);

(iii) A two-electron droplet and a single-electron droplet exchange their positions by transferring an electron from one droplet to the other;

(iv) An empty droplet and a single-electron droplet exchange their positions by transferring an electron from one droplet to the other.

In the linear regime, all these processes contribute to the current density j independently, $j = j_1 + j_2 + j_3 + j_4$. The contributions of the first two processes are

$$j_{1,2} = en_{1,2} \left\langle \sum_i v^i_{1,2} \right\rangle , \qquad (23)$$

where $n_{1,2} = N_{1,2}/V_s$ are the densities of the single- and two-electron droplets, and $\langle ... \rangle$ stands for statistical and time averages. Factors $n_{1,2}$ correspond to electron tunneling from a single-electron droplet (process (i)) or two-electron (ii) droplet. The summation in (23) is performed over all of the magnetic polarons on which the electron can tunnel — one-electron droplets for process (i) and empty droplets for process (ii). Finally, the components of the average electron velocity $\langle v^i_{1,2} \rangle$ along the direction of the electric field are obviously found as [24]:

$$\left\langle \sum_i v^i_{1,2} \right\rangle = \left\langle \sum_i \frac{r^i \cos \theta^i}{\tau_{1,2}(r^i, \theta^i)} \right\rangle , \qquad (24)$$

where r^i and θ^i are the electron tunneling length (the distance between the droplets) and the angle between the electric field and the direction of motion, respectively, and $\tau_{1,2}(r^i, \theta^i)$ are characteristic times associated with the tunneling processes. The relation between $\tau_1(r, \theta)$ and $\tau_2(r, \theta)$ can be found from the following considerations. Near equilibrium, the number of two-electron droplets excited per unit time is equal to the number of decaying two-electron droplets. We thus have the detailed-balance relation,

$$\frac{\overline{N}_1^2}{\tau_1(r, \theta)} = \frac{\overline{N}_2^2}{\tau_2(r, \theta)} , \qquad (25)$$

where we have taken into account that the probability of formation of a two-electron droplet is proportional to the total number N_1 of the single-electron states multiplied by the number of available hopping destinations, which also equals N_1 . Similarly, the probability of decay of a two-electron droplet is proportional to $N_2 N_3 = N_2^2$. Relation (25) implies that $\tau_2(r, \theta) = \tau_1(r, \theta) \exp(-A/k_B T)$. Then we can write the conventional expression for the tunneling times [24] in the form

$$\tau_{1,2}(r, \theta) = \omega_0^{-1} \exp\left(\frac{r}{l} \pm \frac{A}{2k_B T} - \frac{eEr \cos \theta}{k_B T} \right) , \qquad (26)$$

where l and ω_0 are the characteristic tunneling length and magnon frequency, and we have taken into account the contribution of the external electric field to the tunneling probability.

To perform the averaging, we assume that the centers of the magnetic polarons are randomly positioned in space, and the average distance $n^{-1/3}$ between them is much larger than the droplet radius R. Both assumptions seem to be perfectly justified far below the percolation threshold. Then the averaged sum in (23) is essentially the space average of v^i, multiplied by the number of droplets available for hopping (N_1 for the process (i) and N_2 for the process (ii)). Expanding in the small parameter $eEl/k_B T << 1$, we obtain

$$\left\langle \sum_i v^i_{1,2} \right\rangle = \frac{eE\omega_0}{k_B T} N_{1,2} \, e^{-A/2k_B T} \langle r^2 \cos^2 \theta \, e^{-r/l} \rangle_V ,$$

$$\langle ... \rangle_V = V_s^{-1} \int ... \, d^3 r . \qquad (27)$$

In (27) the electric field is outside the averaging. Rigorously speaking, this means that the characteristic hopping length l is larger than the interdroplet distance $n^{-1/3}$, and our approach is valid only when the droplet concentration is not too small. Substituting (27) into (23) and performing the integration, we find

$$j_{1,2} = \frac{32\pi e^2 E \omega_0 l^5 n_{1,2}^2}{k_B T} \exp(\mp A/2k_B T) . \qquad (28)$$

In processes (iii) and (iv) the free energy of the system is not changed after the tunneling, and we write the characteristic times as:

$$\tau_{3,4}(r, \theta) = \omega_0^{-1} \exp(r/l - eEr \cos \theta / k_B T) . \qquad (29)$$

The contribution of these two processes to the current is calculated similarly to that of (i) and (ii). For process (iii) the number of magnetic polarons from which the electron may tunnel is N_2 , whereas the number of accepting droplets is N_1 . In the same way, for process (iv) these numbers are N_1 and $N_3 = N_2$, respectively. Consequently, the factors $n_{1,2}^2$ in (28) are replaced by $n_1 n_2$,

$$j_{3,4} = \frac{32\pi e^2 E \omega_0 l^5 n_1 n_2}{k_B T} . \qquad (30)$$

From (28) and (30) we now obtain the dc conductivity $\sigma = j/E$,

$$\sigma = \frac{32\pi e^2 \omega_0 l^5}{kT} \times$$

$$\times \left[2n_1 n_2 + n_1^2 \, e^{-A/2k_B T} + n_2^2 \, e^{A/2k_B T} \right] . \qquad (31)$$

In this Section, we are only interested in the average conductivity; fluctuations give rise to noise and are considered in Section 6. Using (22), we find that all the four processes illustrated in Fig. 3 give identical contributions to the conductivity; for $A >> k_B T$ the average conductivity (for which we retain the notation σ) reads

$$\sigma = \frac{128\pi e^2 n^2 \omega_0 l^5}{k_B T} \exp(-A/2k_B T) . \qquad (32)$$

We see that the conductivity increases with temperature as $\sigma(T) \propto T^{-1} \exp(-A/2k_B T)$, which is typical for tunneling systems (see, e.g., [24]).

6. $1/f$ noise power

Recently, Podzorov et al. [11] reported the observation of a giant $1/f$ noise in perovskite manganites in the phase-separated regime. Generally, systems with distributed hopping lengths are standard objects which exhibit $1/f$ noise (for review, see Refs. 25, 26). The purpose of this Section is to study low-frequency noise within the framework of the model used to calculate the conductivity in Section 5, and show that it indeed has a $1/f$ form.

Starting from Ohm's law $U = IL/\sigma S$ (where L and S are the sample length and the cross section, respectively) and assuming that the measuring circuit is stabilized (I = const), we can present the voltage noise at the frequency ω, $\langle \delta U^2 \rangle_\omega$, in the following way:

$$\langle \delta U^2 \rangle_\omega = U_{dc}^2 \frac{\langle \delta \sigma^2 \rangle_\omega}{\sigma^2} , \qquad (33)$$

where U_{dc} is the time-averaged voltage, and $\langle \delta \sigma^2 \rangle_\omega$ is the spectrum of conductivity fluctuations.

If we disregard possible fluctuations of the temperature in the system, the only source of fluctuations in our model is those of the occupation numbers n_1 and n_2 . Using the conservation law $n_1 + 2n_2 = n$, we find from (31):

$$\delta\sigma = \sigma \frac{\delta n_2}{n_2} [1 - 2\exp(-A/2k_B T)] . \qquad (34)$$

Now we need to find the fluctuation spectrum $\langle \delta n_2^2 \rangle_\omega$. Taking into account that two-electron droplets decay via process (ii), we can write the relaxation equation in the usual form [27]

$$\delta \dot{n}_2 = -\frac{\delta n_2}{\tau(r)} , \quad \tau(r) = \omega_0^{-1} \exp(r/l - A/2k_B T) , \qquad (35)$$

where we have neglected the effect of the electric field. The fluctuation spectrum then reads [27]

$$\langle \delta n_2^2 \rangle_\omega = \langle \delta n_2^2 \rangle_T \left\langle \sum_i \frac{2\tau(r^i)}{1 + \omega^2 \tau^2(r^i)} \right\rangle =$$

$$= 8\pi \bar{n}_2 \langle \delta n_2^2 \rangle_T \int_0^\infty \frac{\tau(r)}{1 + \omega^2 \tau^2(r)} r^2 dr , \qquad (36)$$

where $\langle \delta n_2^2 \rangle_T$ is the thermal average of the variation of n_2 , and the summation is performed over the «empty droplet—two-electron droplet» pairs, with r_i being the distance between the sites in a pair.

We are interested below in the frequency range

$$\tilde{\omega}_0 \exp(-L_s/l) << \omega << \tilde{\omega}_0 ,$$
$$\tilde{\omega}_0 \equiv \omega_0 \exp(A/2k_B T) , \qquad (37)$$

where L_s is the smallest of the sample sizes. In this case, with logarithmic accuracy we obtain for $A >> k_B T$

$$\langle \delta U^2 \rangle_\omega = U_{dc}^2 \frac{\langle \delta n_2^2 \rangle_T}{\bar{n}_2} \frac{4\pi^2 l^3}{\omega} \ln^2 \left(\frac{\tilde{\omega}_0}{\omega} \right) . \qquad (38)$$

Thus, in a wide range of sufficiently low frequencies (37) the noise power spectrum for our system has almost $1/f$ form.

The variation $\langle \delta n_2^2 \rangle_T = V_s^{-2} (\overline{N_2^2} - \overline{N_2}^2)$ is easily found in the same way as in (22),

$$\langle \delta n_2^2 \rangle_T = \frac{\bar{n}_2}{2V_s} . \qquad (39)$$

Combining this with (38), we write the final expression for the spectral density of noise for $A >> k_B T$ in the form

$$\alpha = \frac{\langle \delta U^2 \rangle_\omega V_s \omega}{U_{dc}^2} = 2\pi^2 l^3 \ln^2 \left(\frac{\tilde{\omega}_0}{\omega} \right). \qquad (40)$$

It is remarkable that the noise spectrum in our model has $1/f$ form down to very low frequencies. This is due to the fluctuations in occupation numbers of droplets, associated with the creation and annihilation of extra electron–hole pairs. This mechanism of $1/f$ noise is specific to our model and is not present in standard hopping conduction [28].

Let us estimate the numerical value of the parameter α, which is the standard measure of the strength of $1/f$ noise. This parameter is proportional to the third power of l. Simple estimates reveal that, in general, l is of the order of or higher than R. Assuming again that the excitation energy is of the order of the Coulomb energy $A \sim e^2/R\varepsilon$, taking ω_0 to be of the order of the Fermi energy inside the droplets (which means $\hbar\omega_0 \sim 300$ K for $n < n_c$), and estimating the tunneling length l as being $l \gtrsim 2R \sim 20$ Å, we arrive to the conclusion that the parameter α is of the order $\alpha \approx 10^{-17}$–10^{-16} cm^3 for $T < A/k_B$ and $\omega \sim 1$ Hz–1 MHz. This value of α is several orders of magnitude higher than in ordinary semiconducting materials (see [25,26]). Such a large magnitude of the noise can be attributed to the relatively low height of the potential barrier A and to the relatively large tunneling length l. Formally, it is also related to the large value of the logarithm squared in (40).

7. Conclusions

Summarizing, we have shown that the narrow-band system, which has the checker-board charge ordering at $n = 1/2$ (corresponding to the doping $x = 0.5$) is unstable toward phase separation away from half-filling ($n \neq 1/2$). It separates into regions with the ideal charge ordering ($n = 1/2$) and other regions in which extra electrons or holes are trapped. The simplest form of these metallic regions could be spherical metallic droplets embedded in the charge-ordered insulating matrix. Simple considerations allow us to estimate the size of these droplets and the critical concentration, or doping $x_c = 1/2 - \delta_c$, at which the metallic phase would occupy the whole sample and the CO phase would disappear. Taking the magnetic interactions into account does not change these conclusions but somewhat modifies the characteristic parameters of the metallic droplets.

The long-range Coulomb interaction may also modify the results, but we do not expect any qualitative changes. For realistic values of the parameters, the size of metallic droplets is still microscopic (about 10–20 Å), and the excess charge in them will be rather small.

The picture obtained corresponds rather well to the known properties of 3D and layered manganites at close to (less than) half doping, $x \leq 1/2$. Our treatment is also applicable to other systems with charge ordering, such as cobaltites [29] and nickelates [30]. It would be interesting to study them for charge carrier concentrations different from the commensurate «checkerboard» one.

A number of important problems still remain unsolved (the origin of the «in-phase» ordering in perovskite manganites in the c direction, the detailed description of inhomogeneous states in the overdoped regime $x > 1/2$, the behavior at finite temperatures). Nevertheless, in spite of the simplifications made, our model seems to capture the essential physics underlying the interplay between phase separation and charge ordering in transition-metal oxides.

Even in our oversimplified model we get reasonable behavior of resistivity for underdoped manganites. Moreover, we have shown that $1/f$ noise appears in the framework of our model in a natural way. The phase separation ensures a large magnitude of the noise power as compared with homogeneous materials. Of course, a more sophisticated theory should include both the ferromagnetic structure of the droplet and the antiferromagnetic structure of the insulating matrix. This can lead us to a physics resembling that observed in the process of spin-assistent tunneling, which attracts a considerable interest nowadays (see, e.g., [31]).

The work was supported by INTAS (grants 97-0963 and 97-11954), the Russian Foundation for Basic Research (projects 00-02-16255 and 00-15-96570) and by the Russian–Dutch Program for Scientific Cooperation. M. Yu. K. acknowledges the support of the Russian President Program (grant 96-15-9694).

1. E. Verwey, *Nature (London)* **144**, 327 (1939); E. Verwey and P. W. Haayman, *Physica* **8**, 979 (1941).
2. T. Mutou and H. Kontani, *Phys. Rev. Lett.* **83**, 3685 (1999).
3. J. van den Brink, G. Khaliullin, and D. I. Khomskii, *Phys. Rev. Lett.* **83**, 5118 (1999).
4. G. Jackeli, N. B. Perkins, and N. M. Plakida, *Phys. Rev.* **B62**, 372 (2000).
5. Z. Jirák, S. Krupička, Z. Šimša, M. Dlouha, and S. Vratislav, *J. Magn. Magn. Mater.* **53**, 153 (1985).
6. A. Arulraj, A. Biswas, A. K. Raychaudhuri, C. N. R. Rao, P. M. Woodward, T. Vogt, D. E. Cox, and A. K. Cheetham, *Phys. Rev.* **B57**, R8115 (1998); M. Uehara, S. Mori, C. H. Chen, and S.-W. Cheong, *Nature (London)* **399**, 560 (1999).

7. E. L. Nagaev, *Usp. Fiz. Nauk* **166**, 833 (1996) [*Sov. Phys. Usp.* **39**, 781 (1996)].
8. A. Moreo, S. Yunoki, and E. Dagotto, *Science* **283**, 2034 (1999).
9. D. Arovas and F. Guinea, *Phys. Rev.* **B58**, 9150 (1998).
10. D. I. Khomskii, *Physica* **B280**, 325 (2000).
11. V. Podzorov, M. Uehara, M. E. Gershenson, T. Y. Koo, and S.-W. Cheong, *Phys. Rev.* **B61**, R3784 (2000).
12. D. I. Khomskii, *Preprint of the P. N. Lebedev Physics Institute*, No. 105 (1969).
13. G. S. Uhrig and R. Vlamink, *Phys. Rev. Lett.* **71**, 271 (1993).
14. P. Pietig, R. Bulla, and S. Blawid, *Phys. Rev. Lett.* **82**, 4046 (1999).
15. M. Yu. Kagan, D. I. Khomskii, and M. V. Mostovoy, *Eur. Phys. J.* **B12**, 217 (1999).
16. S. Mori, C. H. Chen, and S.-W. Cheong, *Nature (London)* **392**, 473 (1998).
17. N. A. Babushkina, L. M. Belova, A. N. Taldenkov, E. A. Chistotina, D. I. Khomskii, K. I. Kugel, O. Yu. Gorbenko, and A. R. Kaul, *J. Phys.: Condens. Mater* **11**, 5865 (1999).
18. M. Hennion, F. Moussa, G. Biotteau, J. Rodríguez-Carvajal, L. Pinsard, and A. Revcolevscki, *Phys. Rev. Lett.* **81**, 1957 (1998).
19. G. Allodi, R. De Renzi, G. Guidi, F. Licci, and M. W. Pieper, *Phys. Rev.* **B56**, 6036 (1997).
20. I. F. Voloshin, A. V. Kalinov, S. E. Savel'ev, L. M. Fisher, N. A. Babushkina, L. M. Belova, D. I. Khomskii, and K. I. Kugel, *Pis'ma Zh. Eksp. Teor. Fiz.* **71**, 157 (2000) [*JETP Lett.* **71**, 106 (2000)].
21. Y. Moritomo, A. Machidas, S. Mori, N. Yamamoto, and A. Nakamura, *Phys. Rev.* **B60**, 9220 (1999).
22. L. Balents and C. M. Varma, *Phys. Rev. Lett.* **84**, 1264 (2000).
23. V. Barzykin and L. P. Gor'kov, *Phys. Rev. Lett.* **84**, 2207 (2000).
24. N. F. Mott and E. A. Davis, *Electronic Processes in Non-Crystalline Materials*, Clarendon Press, Oxford (1979).
25. P. Dutta and P. M. Horn, *Rev. Mod. Phys.* **53**, 497 (1981).
26. Sh. M. Kogan, *Electronic Noise and Fluctuations in Solids*, Cambridge University Press, Cambridge (1996).
27. L. D. Landau and E. M. Lifshitz, *Statistical Physics, Pt. 1*, Butterworth-Heinemann, Oxford (1980).
28. Sh. M. Kogan and B. I. Shklovskii, *Fiz. Tekh. Poluprovodn.* **15**, 1049 (1981) [*Sov. Phys. Semicond.* **15**, 605 (1981)].
29. Y. Moritomo, M. Takeo, X. J. Liu, T. Akimoto, and A. Nakamura, *Phys. Rev.* **B58**, R13334 (1998).
30. J. A. Alonso, J. L. García-Muñoz, M. T. Fernández-Díaz, M. A. G. Aranda, M. J. Martínez-Lope, and M. T. Casais, *Phys. Rev. Lett.* **82**, 3871 (1999).
31. *Tunneling in Complex System*, S. Tomsovic (ed.), World Scientific Singapore (1998).